Piperacillin triggers virulence factor biosynthesis via the oxidative stress response in *Burkholderia thailandensis*

Anran Li[a], Bethany K. Okada[b], Paul C. Rosen[b], and Mohammad R. Seyedsayamdost[a,b,1]

[a]Department of Molecular Biology, Princeton University, Princeton, NJ 08544; and [b]Department of Chemistry, Princeton University, Princeton, NJ 08544

Edited by Caroline S. Harwood, University of Washington, Seattle, WA, and approved May 14, 2021 (received for review October 15, 2020)

Natural products have been an important source of therapeutic agents and chemical tools. The recent realization that many natural product biosynthetic genes are silent or sparingly expressed during standard laboratory growth has prompted efforts to investigate their regulation and develop methods to induce their expression. Because it is difficult to intuit signals that induce a given biosynthetic locus, we recently implemented a forward chemical-genetic approach to identify such inducers. In the current work, we applied this approach to nine silent biosynthetic loci in the model bacterium *Burkholderia thailandensis* to systematically screen for elicitors from a library of Food and Drug Administration–approved drugs. We find that β-lactams, fluoroquinolones, antifungals, and, surprisingly, calcimimetics, phenothiazine antipsychotics, and polyaromatic antidepressants are the most effective global inducers of biosynthetic genes. Investigations into the mechanism of stimulation of the silent virulence factor malleicyprol by the β-lactam piperacillin allowed us to elucidate the underlying regulatory circuits. Low-dose piperacillin causes oxidative stress, thereby inducing redox-sensing transcriptional regulators, which activate *malR*, a pathway-specific positive regulator of the malleicyprol gene cluster. Malleicyprol is thus part of the OxyR and SoxR regulons in *B. thailandensis*, allowing the bacterium to initiate virulence in response to oxidative stress. Our work catalogs a diverse array of elicitors and a previously unknown regulatory input for secondary metabolism in *B. thailandensis*.

antibiotic | natural product | biosynthesis | silent gene cluster | *Burkholderia thailandensis*

Since the discovery of penicillin in 1928, antibiotics have served as essential weapons in the fight against infectious disease. Much like penicillin, 70% of today's clinical antibiotics are based on naturally occurring molecules referred to as natural products or secondary metabolites (1, 2). Natural products are synthesized by dedicated biosynthetic gene clusters (BGCs), sets of often contiguous genes found in all kingdoms of life. Importantly, under standard laboratory growth conditions, most microbial BGCs are sparingly expressed or transcriptionally silent, and their cognate products do not accumulate to detectable levels (3–7). Also referred to as cryptic, these BGCs constitute a major reservoir of new molecules, and methods that can access their products would benefit natural product discovery and allied fields.

The opportunity provided by silent BGCs has been recognized by the research community, and several methods have been developed for activating them (8–13). We recently added a forward chemical-genetics strategy, termed high-throughput elicitor screening (HiTES), to the cadre of available approaches (14). In HiTES, a reporter gene is inserted into a silent BGC of interest, affording a facile expression read-out. Elicitors (i.e., compounds that induce expression of the chosen BGC) are then selected from a library of small molecules via high-throughput screening. With the elicitor identified, the product of the silent BGC and its regulation can be investigated. We have applied HiTES and variations thereof to diverse bacteria and uncovered numerous elicitors and dozens of cryptic metabolites, some more potent than clinically used therapies (15, 16). Yet it remains challenging to find a "magic bullet" to broadly activate secondary metabolism in a host. Moreover, other than a few exceptions, the mechanisms by which elicitors turn on silent BGCs remains unknown. Many identified elicitors are cytotoxins, which kill at high concentrations but stimulate secondary metabolism at low titers (14–19). The molecular basis underlying this hormetic effect has yet to be determined (20–25).

Herein, we address these topics using *Burkholderia thailandensis*, a naturally occurring saprophyte and an avirulent representative of the Pseudomallei group pathogens that has emerged as a model for the regulation and synthesis of cryptic metabolites (26, 27). *B. thailandensis* encodes at least 22 BGCs, of which 3 are expressed at detectable levels under standard conditions in the laboratory (28–31). The remaining 19 BGCs are silent or sparingly expressed. To identify elicitors, we applied HiTES to nine silent BGCs in *B. thailandensis* using a library of 770 Food and Drug Administration (FDA)–approved compounds. The structurally diverse elicitors that we identified suggest the presence of multiple mechanisms for inducing secondary metabolism and provide the basis for dissecting regulatory inputs for cryptic BGCs. Sublethal doses of β-lactam antibiotics were especially effective at eliciting secondary metabolism. We focused on the induction of the silent virulence factor malleicyprol by piperacillin (pip) as a model for how β-lactams induce secondary metabolism. We found that low-dose pip triggers

Significance

Low-dose antibiotics can activate the expression of otherwise silent biosynthetic loci, but the mechanisms underlying this phenomenon are poorly understood. Our results reveal several classes of molecules that globally induce secondary metabolite biogenesis in the model bacterium *Burkholderia thailandensis*. We illuminate the mechanism of induction of one of these elicitors, the β-lactam piperacillin, and uncover oxidative stress as a new input that initiates synthesis of the virulence factor malleicyprol. The finding that malleicyprol is a component of the oxidative stress response indicates that *B. thailandensis* has evolved to trigger virulence when faced with reactive oxygen species. Understanding the links between small-molecule elicitors and otherwise silent biosynthetic programs promises to unlock the structures and regulation of so-far "hidden" natural products.

Author contributions: A.L., B.K.O., P.C.R., and M.R.S. designed research; A.L., B.K.O., and P.C.R. performed research; A.L., B.K.O., P.C.R., and M.R.S. contributed new reagents/analytic tools; A.L., B.K.O., P.C.R., and M.R.S. analyzed data; and A.L., P.C.R., and M.R.S. wrote the paper.

The authors declare no competing interest.

This article is a PNAS Direct Submission.

See online for related content such as Commentaries.

[1]To whom correspondence may be addressed. Email: mrseyed@princeton.edu.

This article contains supporting information online at https://www.pnas.org/lookup/suppl/doi:10.1073/pnas.2021483118/-/DCSupplemental.

Published June 25, 2021.

oxidative stress, which, in turn, activates the transcriptional regulators OxyR and SoxR that induce malleicyprol synthesis through *malR*, a cluster-specific LuxR-type transcriptional activator of the malleicyprol BGC. This work therefore harnesses a chemical screen to reveal a previously unappreciated role for oxidative stress in regulating a silent biosynthetic cluster in *B. thailandensis*.

Results

Expanded Screens Reveal Inducers of Silent BGCs. While previous iterations of HiTES in *B. thailandensis* helped to uncover new secondary metabolites and inducing stimuli, they focused on just 2 of 19 silent BGCs (14, 32). We sought to obtain a broader view of elicitors of secondary metabolism in *B. thailandensis* and applied HiTES to nine silent BGCs (*SI Appendix*, Table S1 and Fig. S1), including the *mal*, *org*, and *mba* clusters as well as six other BGCs with unknown products. Upon low-dose antibiotic treatment, the *mal* BGC gives rise to the cytotoxin malleicyprol, which spontaneously converts to malleilactone and its tautomer burkholderic acid (Fig. 1*A*) (33–35). The *mal* BGC is necessary for Pseudomallei group pathogenicity in *Caenorhabditis elegans* infection models (33). The target and mechanism of action of malleicyprol, however, remain to be determined. The *org* cluster is responsible for the synthesis of thailandenes, polyene natural products that exhibit antibacterial activity against Gram-positive strains (36). Like *mal* and *org*, the *mba* locus is conserved in the Pseudomallei complex within the *Burkholderia* genus and directs the synthesis of the siderophore malleobactin (Fig. 1*A*) (37). The *tomm* cluster codes for a putative thiazole–oxazole modified microcin; its product is not known (38). The products of the remaining five BGCs also await discovery; antiSMASH-based bioinformatic predictions suggest that they code for diverse structural classes of secondary metabolites (39) (*SI Appendix*, Fig. S1).

For each BGC, we selected a translational LacZ fusion from the sequence-defined *lacZ* insertion library created by the Manoil laboratory (40). Each strain was screened against a 770-member FDA-approved drug library. For each screen, we used a translational LacZ fusion to BtaK in the bactobolin gene cluster, which is expressed at high cell densities, as a positive control and the reporter strain for the silent BGC in the absence of any compounds as the negative control. The results were normalized based on the fold change versus the negative control, combined, and colorized to produce an elicitor heat map showing how the expression of each of the nine silent BGCs changes in response to 770 FDA-approved drugs (Fig. 1*B*). The data were clustered based on the mode of action of each candidate elicitor to facilitate identification of families of inducers of silent BGCs in *B. thailandensis*.

A number of features emerge from this heat map. Six families of FDA drugs, including over 40 different compounds, were identified as general elicitors. Of these, three were antibiotics: the β-lactams, fluoroquinolones, and ergosterol synthesis inhibitors. Notably, β-lactams, which are used to treat *Burkholderia* infections, were among the most active stimulators in our dataset (41, 42). But our screen surprisingly also uncovered nonantibiotics that broadly activated silent BGCs, including clinical antipsychotics that target dopamine receptors, antidepressants that inhibit serotonin reuptake, and calcimimetics. Within each family, apparent structure–activity relationships (SARs) could be observed, as some members failed to elicit, while others broadly induced silent BGCs (Fig. 1*B*, see next section). We independently validated one representative member from each elicitor family and observed, consistent with the screening results, 5- to 500-fold induction of the BGCs tested (*SI Appendix*, Fig. S2). Representative compounds within each family of elicitors are shown (Fig. 1*C*). That such a diverse set of structural chemotypes activates expression of silent BGCs suggests distinct mechanisms of induction. Our heat map

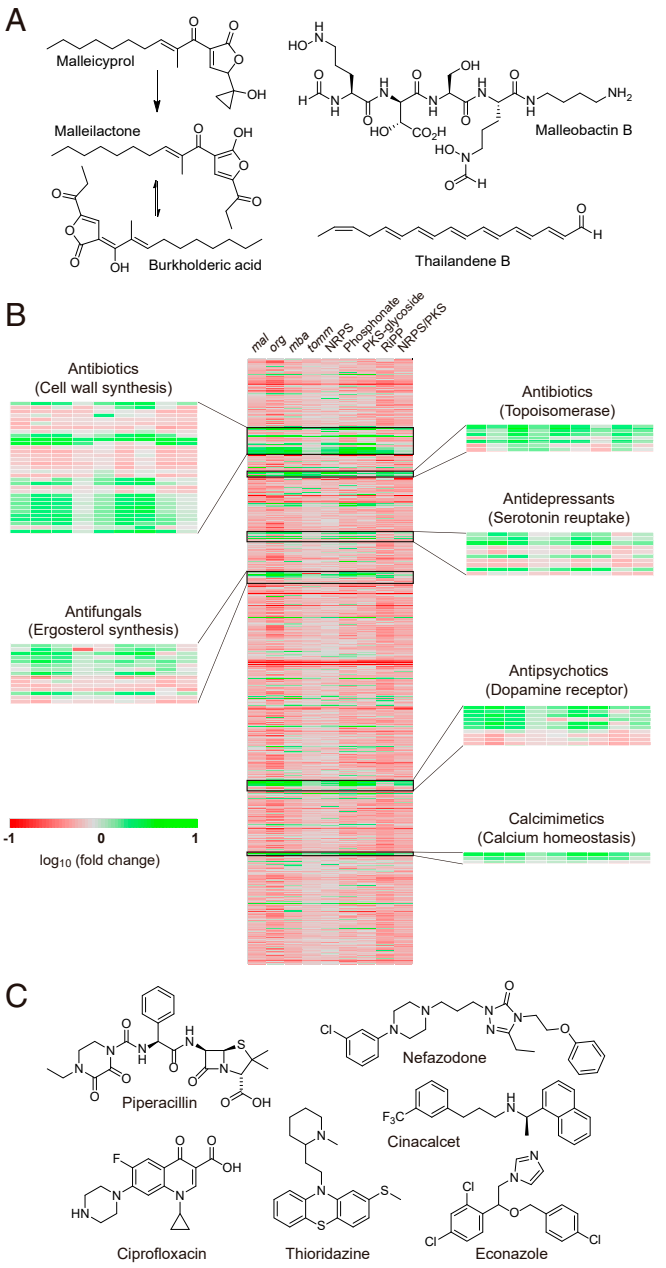

Fig. 1. Drug molecules activate silent BGCs in *B. thailandensis*. (*A*) Products of the *mal*, *org*, and *mba* gene clusters in *B. thailandensis*. (*B*) The expression of nine silent BGCs was measured in response to a 770-member FDA-approved drug library. The BGCs are labeled in each column. Compound families that broadly induced the selected BGCs are highlighted. The color bar indicates the observed fold changes. (*C*) Structures, drug category, and target of representative inducers: pip (antibiotic, cell wall), ciprofloxacin (antibiotic, topoisomerase), thioridazine (antipsychotic, dopamine receptor), cinacalcet (calcium homeostasis, Ca^{2+}-sensing receptors), nefazodone (antidepressant, serotonin reuptake), econazole (antifungal, ergosterol synthesis).

provides a useful resource of relevant FDA-approved drugs that modulate secondary metabolism in *B. thailandensis*.

β-Lactam–Mediated Induction of Secondary Metabolism Requires Antibiosis. The β-lactam family was well represented in our drug library, containing several penicillins, penems, and a large subfamily of 19 cephalosporins. The comprehensive cephalosporin coverage allowed us to conduct an SAR analysis. While first-generation cephalosporins were incapable of inducing the

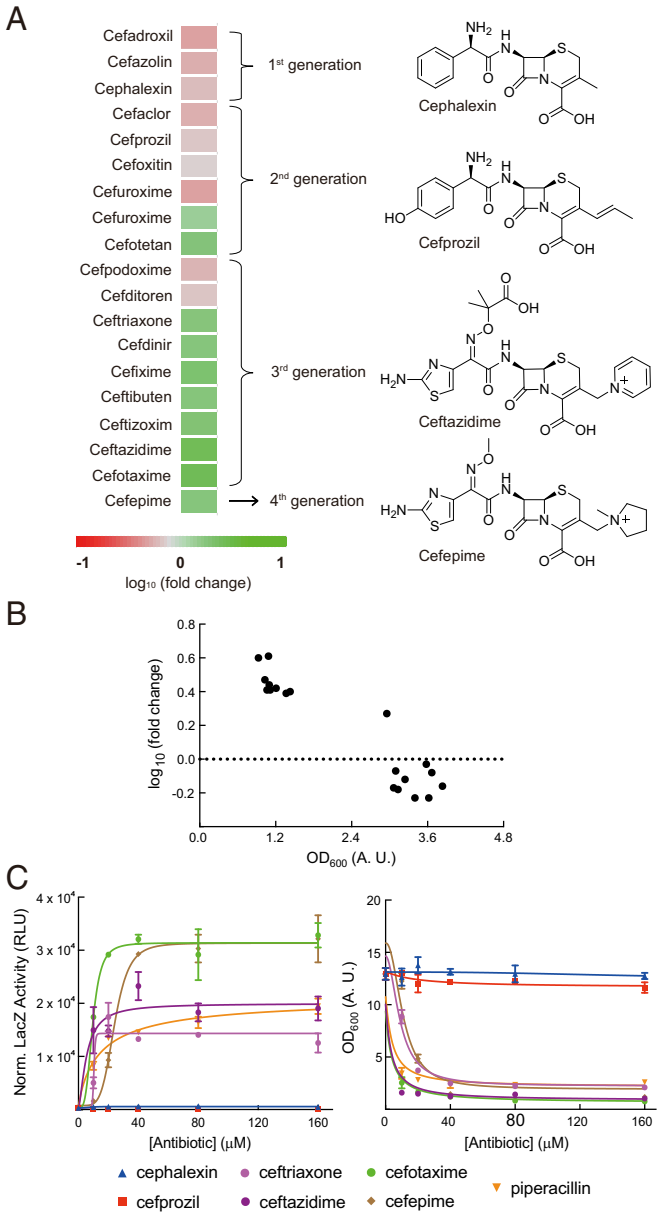

Fig. 2. Antibiosis is required for induction of the *mal* BGC by β-lactam antibiotics. (*A*) Structure–activity relationship between cephalosporins and elicitor activity. The data from the heat map in Fig. 1*B* are reorganized according to cephalosporin generation; structures of representative members are shown. (*B*) Correlation between growth inhibition and elicitation of *mal* for cephalosporins in the drug library. (*C*, *Left*) OD_{600}-normalized elicitation dose response for select β-lactams as measured with a *malA-lacZ* reporter. Note that cephalexin and cefprozil result in ~1,500 relative light units (RLUs), similar to the vehicle control. (*Right*) Growth-inhibition assays with the same β-lactams determined spectrophotometrically at 600 nm (OD_{600}). The averages of three independent replicates are shown; bars represent SE. A. U., absorbance unit with a 1-cm pathlength.

mal BGC, third- and fourth-generation drugs generally exhibited the strongest induction (Fig. 2*A*). The cephalosporins mapped into two categories (Fig. 2*B*), those that inhibited the growth of *B. thailandensis* and increased *mal* expression or those that had neither effect. One outlier (cefuroxime) had a moderate effect on both phenotypes. Together, these results point to a clear correlation between the ability of cephalosporins to inhibit *B. thailandensis* growth and induce the *mal* BGC.

We selected representative member(s) from each cephalosporin generation and determined the half-maximal growth-inhibitory concentration (IC_{50}) as well as the half-maximal elicitor concentration (EC_{50}) for inducing the *mal* BGC. First- and second-generation cephalosporins, such as cephalexin and cefprozil, exhibited low/no toxicity and failed to induce *mal*. By contrast, third- and fourth-generation drugs ceftriaxone, ceftazidime, cefotaxime, and cefepime, as well as pip, showed low half-maximal inhibitory concentrations (IC_{50}s between 2 and 17 μM) and effective stimulation of the *mal* BGC with half-maximal elicitation concentrations in the same range (9 to 24 μM, Fig. 2*C* and *SI Appendix*, Table S2). These results indicate that *mal* induction by β-lactams not only correlates with but is dependent on antibiosis, thus linking toxicity to stimulation of secondary metabolism. Furthermore, even though all the β-lactams tested are structurally very similar, only the subset that impedes growth can induce the *mal* BGC, suggesting that the stimulatory effect is mediated through the canonical role of interfering with cell-wall biosynthesis rather than through off-target effects. We focused on the mechanism of elicitation by pip because it was among the best inducers of silent BGCs and is used to treat *Burkholderia* infections (41). Further experiments with pip were carried out at 10 μM, threefold lower than the minimal inhibitory concentration (MIC) of this antibiotic against *B. thailandensis*. A growth curve and *mal* expression time course indicated optimal induction at ~12 h (*SI Appendix*, Fig. S3).

Pip Triggers Production of Reactive Oxygen Species. In *Escherichia coli*, inhibitory concentrations of the β-lactam ampicillin (Amp) have been proposed to generate reactive oxygen species (ROS) and to underlie the cidal properties of the antibiotic. Some evidence also suggests that β-lactam treatment results in ROS production in *Pseudomonas aeruginosa*, *Vibrio cholerae*, and other bacteria (25, 43–46). We therefore tested whether low-dose pip treatment in *B. thailandensis* results in a similar fate.

ROS are small, reactive, and difficult to detect directly. Induction of the oxidative stress response serves as a reliable proxy for the presence of ROS (47, 48). Specifically, H_2O_2 induces OxyR activity at the protein level through oxidation of a pair of cysteine residues to a disulfide. The oxidized OxyR then induces expression of a regulon that includes antioxidant enzymes such as catalase (*katG*) and alkylhydroperoxide reductase (*ahpCD*), iron chelators to soak up unincorporated iron, manganese import proteins, disulfide reductases, DNA and protein repair enzymes, and other genes. Another important redox-dependent transcriptional regulator, SoxR, carries a [2Fe-2S] cluster and can be activated by redox-active compounds (49, 50); the oxidized form of SoxR induces a regulon that only partially overlaps with that of OxyR in *E. coli*. Using RT-qPCR, we observed 2- to 4-fold induction of *ahpCD* and 11-fold induction of *katG* upon low-dose pip treatment of *B. thailandensis* (Fig. 3*A*). Importantly, this induction was entirely OxyR-dependent, as a deletion mutant (Δ*oxyR*, *SI Appendix*, Table S1) did not induce these genes in response to pip. A similar response was detected with the well-known ROS inducers plumbagin and menadione (*SI Appendix*, Fig. S4).

In *E. coli*, H_2O_2-mediated stress results in stimulation of enterobactin biosynthesis (51), and we therefore investigated production of iron-scavenging agents as further indication of oxidative stress. *B. thailandensis* synthesizes the siderophores pyochelin and malleobactin, respectively encoded by the *pch* and *mba* BGCs (37). Using available *mbaC-lacZ* and *mbaM-lacZ* reporters, we detected 2.5- to 3-fold induction by low-dose pip as well as various degrees of induction by well-known ROS inducers (*SI Appendix*, Fig. S5*A*). RT-qPCR revealed nearly 80-fold induction of *pchE*, an effect that was largely OxyR-dependent (*SI Appendix*, Fig. S5*B*). Together, the effects on *ahpCD*, *katG*, *mba*, and *pch* suggest that low-dose pip causes oxidative stress in *B. thailandensis*.

We explored three additional lines of evidence for the presence of ROS. First, using a fluorescent reporter dye (45), which

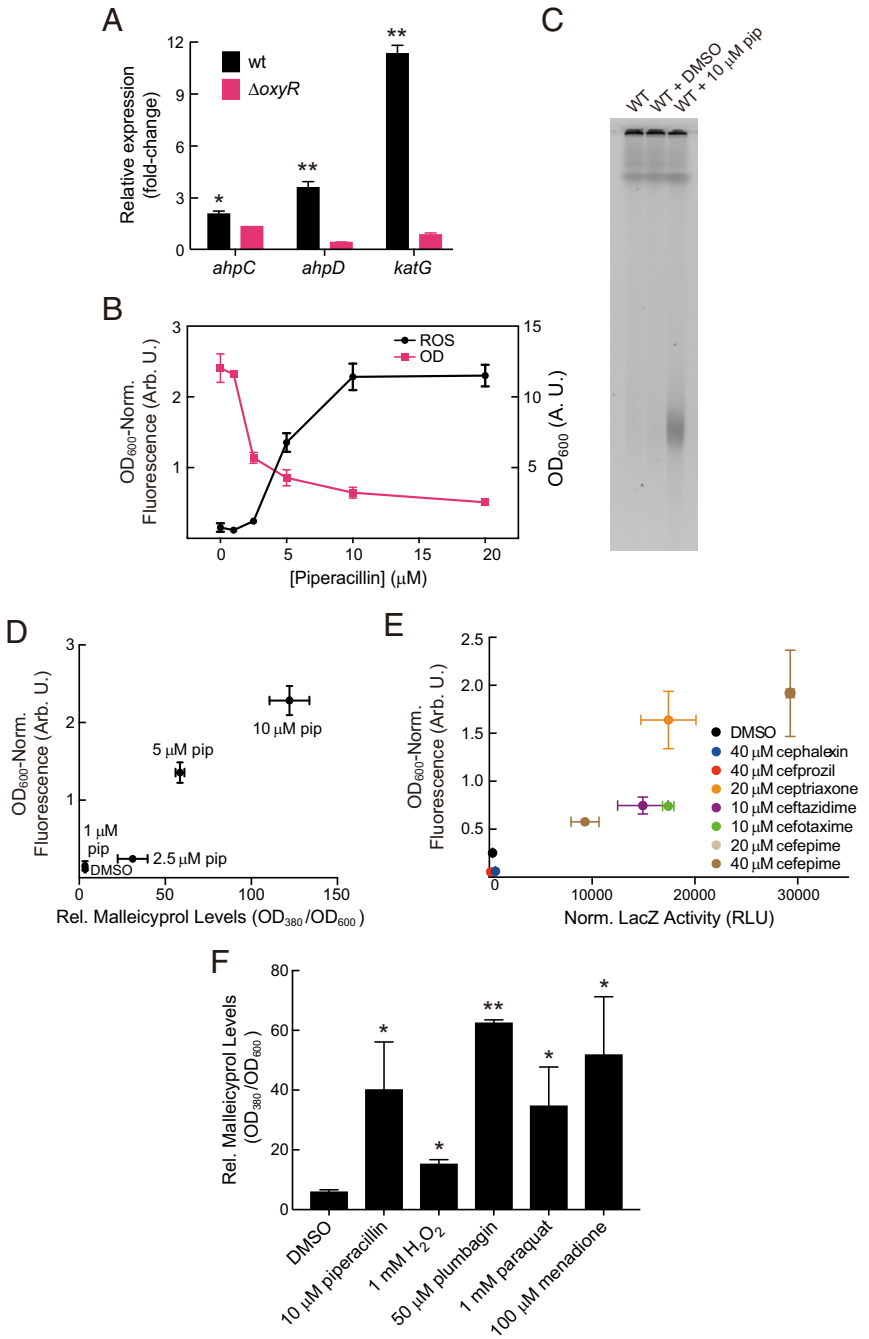

Fig. 3. Low-dose pip induces ROS. (*A*) Expression of *ahpCD* and *katG* as determined by RT-qPCR in wt and *ΔoxyR B. thailandensis* upon low-dose pip treatment. *P* values indicate comparison to the same strain under vehicle treatment. (*B*) ROS production, measured using an ROS-sensitive fluorescent dye (black trace), and growth inhibition, measured spectrophotometrically at 600 nm (OD_{600}, pink trace), as a function of pip dose. (*C*) Low-dose pip leads to double-stranded breaks as gauged by PFGE to visualize genomic DNA. (*D*) Correlation of ROS levels and malleicyprol biosynthesis, as determined by HPLC–MS analysis, as a function of pip concentration. (*E*) ROS levels normalized for OD_{600} are correlated with *mal* BGC induction as measured by normalized LacZ activity (Pearson correlation $R^2 = 0.81$, $P < 0.002$). (*F*) Production of malleicyprol, as measured by HPLC–MS, in response to H_2O_2 and well-established ROS inducers. *P* values indicate comparison to the same strain under vehicle treatment. In all panels, the averages of three independent replicates are shown. Error bars represent SE; *P* values determined by Student's two-tailed *t* test (*$P < 0.05$ and **$P < 0.01$) are indicated.

has been employed by several groups and monitors hydroxyl radicals (HO•s) and, by extension, related ROS that give rise to HO•, we detected a dose-dependent turn-on fluorescence signal as a function of pip (Fig. 3*B*). At 10 μM, 30-fold higher ROS levels were detected relative to vehicle control. ROS levels correlated with the extent of growth inhibition induced by pip (Fig. 3*B*). Malleicyprol itself did not trigger fluorescence from the dye as control experiments show; moreover, no autofluorescence was observed in the absence of the dye (*SI Appendix*, Fig. S6). Second, using pulsed-field gel electrophoresis (PFGE) and terminal deoxynucleotidyl transferase dUTP nick-end labeling (TUNEL), we observed that pip treatment in *B. thailandensis* causes DNA

damage, a hallmark consequence of ROS, notably HO•s (Fig. 3*C* and *SI Appendix*, Fig. S7) (52–54). Finally, and consistent with this latter result, RT-qPCR showed that some repair and biosynthesis pathways were mildly induced. These included 1.6- to 8-fold induction of select genes in the SOS DNA-damage regulon (*recA*, *lexA*, *uvrA*, and *dinB*), twofold repression of *ftsZ* expression, and low-level induction of certain DNA and cell-wall biosynthesis genes (*SI Appendix*, Fig. S8 *A* and *B*) (55, 56). Importantly, a *recA* delection mutant (Δ*recA*) was found to be synthetic lethal in the presence of low-dose pip (*SI Appendix*, Fig. S8*C*). Together, these results demonstrate the presence of ROS and ROS-mediated DNA damage upon pip treatment.

H_2O_2 and ROS Inducers Trigger Malleicyprol Synthesis. To investigate whether ROS production underpins induction of secondary metabolism, we simultaneously measured ROS levels and malleicyprol biosynthesis. A clear correlation was observed when investigating different doses of pip (Fig. 3*D*). In addition, six cephalosporins of varying potencies also showed correlated ROS induction and *mal* cluster activation: cefprozil and cephalexin barely activated ROS and the *mal* cluster, whereas cefepime caused high levels of ROS and malleicyprol biosynthesis (Fig. 3*E*).

We also tested the effects of H_2O_2 and ROS inducers on malleicyprol production (Fig. 3*F*). A final concentration of 1 mM H_2O_2 led to threefold induction of malleicyprol synthesis, whereas 4 mM were lethal. Even better induction was observed with a series of well-known inducers of ROS, including plumbagin, paraquat, and menadione (57, 58). Plumbagin (at 50 μM) and menadione (at 100 μM) yielded 9- to 11-fold higher malleicyprol titers relative to vehicle control. Low-dose pip resulted in a similar level of malleicyprol synthesis as 1 mM paraquat. The induction of malleicyprol biosynthesis in response to H_2O_2 and ROS inducers validates ROS as a mechanistic link between β-lactam treatment and activation of the silent *mal* cluster.

Pip Requires Redox-Sensitive Transcriptional Regulators and MalR to Induce the *mal* BGC. We next interrogated the involvement of redox-sensitive transcriptional regulators in the pip-mediated secondary metabolite response by testing the ability of deletion mutants Δ*oxyR* and Δ*soxR* to trigger malleicyprol biosynthesis. Although the mutants grew similarly to the wild type (wt) in the presence and absence of pip, both strains exhibited reduced malleicyprol synthesis (64% and 40%, respectively) in response to the antibiotic; these effects were rescued by plasmid-encoded expression of *oxyR* in the Δ*oxyR* strain and of *soxR* in the Δ*soxR* strain (Fig. 4*A* and *SI Appendix*, Fig. S9*A*). In agreement, reduced LacZ activity was detected in the reporter constructs Δ*oxyR-malA-lacZ* and Δ*soxR-malA-lacZ* upon pip treatment when compared with the parent wt reporter *malA-lacZ* (*SI Appendix*, Fig. S9*B*). Notably, a double deletion of *soxR* and *oxyR* (Δ*oxyR*Δ*soxR*) completely abrogated the pip-mediated malleicyprol induction effect (Fig. 4*A*). By contrast, trimethoprim (Tmp), a well-known inducer of secondary metabolism and an antibiotic with a different mode of action, triggered malleicyprol production similarly in wt, Δ*oxyR*, Δ*soxR*, and Δ*oxyR*Δ*soxR* double knockout strains (*SI Appendix*, Fig. S9*C*) (14, 19). These results suggest that OxyR is not generally involved in malleicyprol induction but rather is required specifically in response to oxidative stress. These findings suggest that OxyR and SoxR provide the major pathway for control of *mal* induction under conditions of oxidative stress mediated by pip.

It has previously been shown that production of malleicyprol relies on the pathway-specific LuxR-type regulator MalR (59). Interestingly, analysis of the *malR* promoter region revealed two sequences at −19 bp and −386 bp, which are homologous to the canonical *oxyR* binding site in *B. thailandensis* (Fig. 4*B*), suggesting that *malR* may be directly induced by OxyR (56, 60). A Δ*malR* strain exhibited no growth defects and had similar levels of ROS compared to wt, but its ability to synthesize malleicyprol in response to pip was completely abolished as indicated by HPLC–MS analysis (Fig. 4*C* and *SI Appendix*, Fig. S9 *D* and *E*). MalR is therefore required for pip-mediated induction of malleicyprol synthesis, though malleicyprol is not required for surviving pip treatment or suppressing ROS.

We tested whether OxyR can directly bind the *malR* promoter region with electrophoretic mobility shift assays (EMSAs). Using the 670-bp promoter sequence of *malR*, we observed an OxyR-dose–dependent mobility shift, consistent with the formation of a DNA–protein complex (Fig. 4*D*). A similar result was obtained using the promoter region of AhpC, which is known to be induced by oxidative stress in *B. thailandensis* (61). By contrast, an arbitrary DNA sequence did not exhibit a shift with high concentrations of OxyR (Fig. 4*D*). Moreover, OxyR did not bind to a similar DNA fragment, in which the sequence of the two OxyR binding sites had been scrambled (*SI Appendix*, Fig. S10).

We next tested whether OxyR and SoxR activate *malR* expression. First, *E. coli* cells were transformed with a plasmid encoding arabinose-inducible *B. thailandensis oxyR* and a promoter–reporter construct comprised of the *malR* promoter and the *lacZ* reporter. Growth of the *E. coli* strain and subsequent arabinose-dependent induction of *oxyR* revealed a dose-dependent increase in LacZ activity. At the highest concentration of arabinose, a threefold increase in LacZ activity was observed (Fig. 4*E*). A similar profile was observed in the positive control, in which the promoter region of *ahpC* was substituted in place of the *malR* promoter sequence. Moreover, the Δ*oxyR* and Δ*soxR* strains induced *malR* in the presence of pip to a lesser extent than wt *B. thailandensis* as assessed with RT-qPCR; deletion of both *soxR* and *oxyR* completely abolished pip-dependent *malR* up-regulation (Fig. 4*F*). Note that the levels of *malR* induction observed are consistent with prior work; Tmp, an established strong elicitor of the *mal* cluster, induces *malR* ∼2.5- to 3-fold (19). Together, the results in Fig. 4 support a model wherein pip generates oxidative stress that activates redox-sensitive transcriptional regulators, which then up-regulate MalR to induce the production of malleicyprol.

Discussion

That the effects of antibiotics are highly concentration dependent is well documented. Low doses can have diverse, nonlethal effects such as cell-wide transcriptional reprogramming and alteration of biofilm formation and quorum sensing (20–24). The induction of otherwise silent natural product BGCs by low-dose antibiotics is an emerging dimension of the idea that antibiotics can exert effects other than growth inhibition or cell death (14, 24, 62). However, the mechanisms underlying this phenomenon have been poorly understood. The current work innovates in two important aspects to address this issue. It identifies new activating inputs of secondary metabolism, and it delineates the mechanism by which one of these signals activates silent BGCs.

We show that the oxidative stress response, mediated by pip treatment, can induce expression of the *mal* BGC and lead to synthesis of the malleicyprol virulence factor (Fig. 5). Our work aligns with the notion that antibiotics exert physiologically important functions through ROS (63, 64). The source of pip-induced ROS remains to be determined; possible candidates include the electron-transport chain and spurious reaction of O_2 with enzymes that carry accessible metallocofactors (47, 48). One particular dilemma with pip is that both removal of ROS and repair processes, which are triggered in response to inhibition of cell-wall biosynthesis (65, 66), require reducing equivalents. It is conceivable that this demand results in a cycle of ROS formation and/or an inability to effectively remove ROS, ultimately leading to the response that we catalog herein.

At low doses of pip, *B. thailandensis* mounts a secondary metabolite response in which silent BGCs are broadly activated as our current results show. The biosynthesis of malleicyprol may represent a defense measure but likely not an antioxidant response

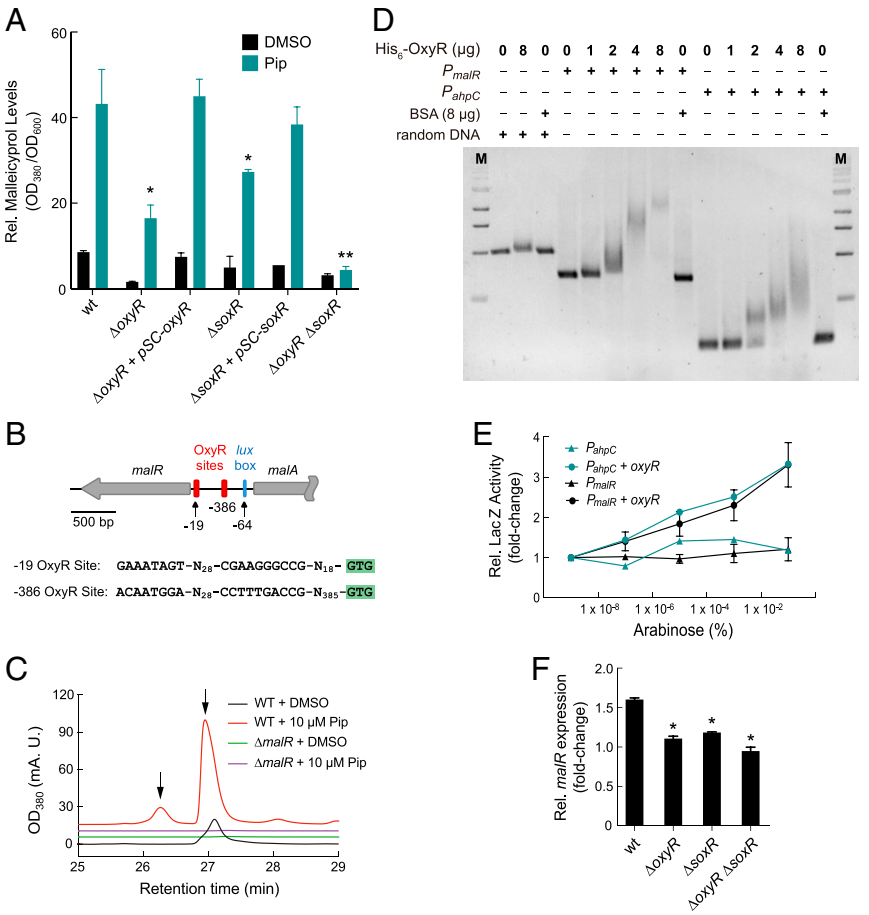

Fig. 4. Pip requires redox-sensitive transcriptional regulators to activate the *mal* BGC through MalR. (*A*) OxyR and SoxR are required for pip-mediated malleicyprol biosynthesis, as measured by HPLC–MS. *P* values indicate comparison to the wt strain under low-dose pip treatment. (*B*) Two OxyR binding sites (red) can be identified in the *malR* promoter region as well as a *lux* box (blue) upstream of *malA*. The sequences of the putative OxyR binding sites are shown in the 5′ to 3′ direction; GTG (green) designates the MalR start codon. (*C*) MalR is required for pip to induce malleicyprol production, as gauged by HPLC–MS. The arrows point to malleilactone variants B (*Left*) and A (*Right*). (*D*) EMSAs show that OxyR binds to the *malR* promoter region and to the positive control *ahpC* promoter region but not to an arbitrary DNA sequence. Conditions are indicated above each lane; M, marker. See also *SI Appendix*, Fig. S10. (*E*) Induction of *malR* by OxyR. *E. coli* cells were transformed with a plasmid encoding *lacZ* under the control of the *malR* promoter or the *ahpC* promoter as well as an arabinose-inducible *B. thailandensis* OxyR. LacZ activity was measured upon induction and compared with the lowest arabinose concentration to show fold induction. (*F*) *malR* expression in wt and indicated *B. thailandensis* mutants determined by RT-qPCR upon low-dose pip treatment, normalized to a vehicle control. *P* values indicate comparison to wt strain under low-dose pip treatment. The averages of three independent replicates are shown in *A*, *E*, and *F*. Error bars represent SE; *P* values determined by Student's two-tailed *t* test (*$P < 0.05$ and **$P < 0.01$) are indicated.

(*SI Appendix*, Fig. S9 *D* and *E*). Mechanistically, *mal* induction depends on the redox-sensitive transcriptional regulators OxyR and SoxR, whose activities are induced by H_2O_2 and redox-active metabolites, respectively (56). Our analysis of deletion mutants suggests that OxyR and, to a lesser extent, SoxR provide the main pathways for induction of the *mal* BGC (Figs. 4 and 5). Details regarding the regulation of *mal* by SoxR remain to be elucidated. With OxyR, we show direct binding to the *malR* promoter, leading to induction of the *mal*-specific transcriptional activator MalR, which results in malleicyprol biogenesis. Malleicyprol synthesis is thus activated by the oxidative stress response. The extent to which this model is conserved in related *Burkholderia* species remains to be investigated, but it would predict that ROS resulting from phagocytosis by immune cells during infection or from β-lactams in environmental encounters with fungi could, in these contexts, make *Burkholderia* more virulent via stimulation of malleicyprol production (41, 67, 68).

The ability of compounds that cause oxidative stress to induce cryptic natural product synthesis likely extends beyond the case of pip and the *mal* BGC in *B. thailandensis*. Redox-sensitive transcriptional regulators have been proposed as activators of secondary metabolite biosynthesis in diverse bacteria including streptomycetes and *Bacillus subtilis* (69–72). The idea that oxidative stress could be a general stimulus for silent BGCs is tantalizing, as it could empower systematic discovery efforts for cryptic natural products and their regulation. Interestingly, some antibiotics function through perturbing the redox balance; the question of how reducing equivalents are allocated to remove ROS and, at the same time, contribute to secondary metabolism, remains to be answered (63, 64, 67, 73). Reducing equivalents provide a key link between primary and secondary metabolism, and exploring this link in the context of oxidative stress in BGC-rich bacteria provides avenues for future research.

An additional broader implication relates to the molecular basis of hormesis (20, 21). Inhibitory levels of pip are proposed to kill via cell-wall disruption and subsequent ROS stress; low doses elicit secondary metabolism via the same mechanism. Likewise, Tmp is an antimetabolite that kills via inhibition of dihydrofolate reductase (19); low-dose Tmp acts via the same target to turn on silent BGCs. ARC-2, a triclosan-like synthetic analog, induces secondary metabolism in *Streptomyces coelicolor* via inhibition of fatty acid synthesis (17); triclosan kills via the

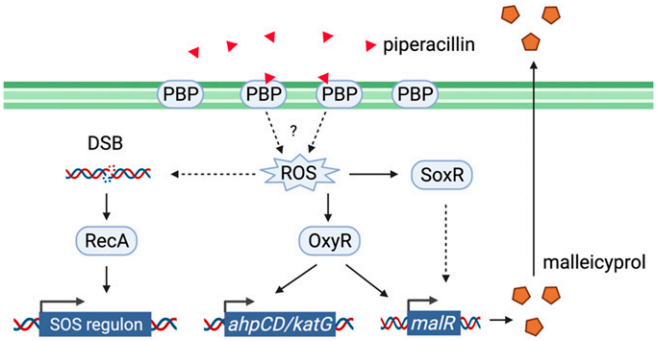

Fig. 5. A model for the pip-mediated activation of the *mal* gene cluster in *B. thailandensis*. Low-dose pip treatment results in production of ROS by yet-unknown mechanisms. ROS generate double-stranded DNA breaks (DSB), inducing the SOS response via RecA. They also induce SoxR and OxyR, which trigger the oxidative stress response. OxyR activates the canonical OxyR regulon genes including *ahpCD* and *katG*. It also induces *malR* expression by binding to an upstream promoter region. MalR then triggers expression of the *mal* gene cluster, which results in malleicyprol and malleilactone biosynthesis.

same mechanism. The hormetic response to these antibiotics, therefore, is governed by partial versus complete inhibition of the target and the associated consequences. Partial inhibition allows bacteria to reorganize resources (i.e., reducing equivalents, precursor molecules) to mount a counterattack, whereas complete or near-complete inhibition drains resources leading to the cell's demise. Combining the two lines of reasoning above, one simple approach to find elicitors would be to screen for antibiotics that a given bacterium is susceptible to at inhibitory doses. Low titers of that same antibiotic would be a candidate elicitor for induction of silent BGCs.

Beyond revealing oxidative stress as an activating input for secondary metabolism, our work also provides a resource for discovering the molecules produced by silent BGCs in *B. thailandensis* (Fig. 1*A* and *SI Appendix*, Fig. S1). Identifying small-molecule inducers and their corresponding products will help derive a global picture of secondary metabolism and its modulation by exogenous molecules (16, 74). Many commonly prescribed drugs, including nonantibiotics like antipsychotics, have increasingly been appreciated as important determinants of the composition and function of the human microbiome through mechanisms that remain largely unknown (75, 76). Our screen, which systematically studied the effects of FDA-approved drugs in activating a large panel of cryptic BGCs in *B. thailandensis*, points unexpectedly to low doses of antipsychotic and antidepressant drugs as potent, general BGC inducers (Fig. 1). These drugs, therefore, could activate cryptic BGCs in constituents of the human microbiome, potentially providing an explanation for their surprising regulatory effects. Elucidating the underlying mechanisms would lead to a better understanding of small-molecule relays important in physiology and disease.

Materials and Methods

Bacterial Strains and Growth Conditions. *B. thailandensis* E264 was obtained from the American Type Culture Collection and used throughout this study. It was routinely cultured in LB-MOPS, which consists of Lysogeny Broth (LB, Becton-Dickinson) supplemented with 50 mM MOPS (Fisher), with the pH adjusted to 7.0 using NaOH. *E. coli* DH5-α was used for common plasmid construction and amplification. *E. coli* JV36, used as a conjugal donor, was kindly provided by Joshua A. V. Blodgett (Department of Biology, Washington University, St. Louis, MO) (77). *E. coli* strains were routinely grown in LB broth at 37 °C and 200 rpm in 14-mL bacterial culture tubes. All antibiotics were obtained from Sigma-Aldrich or Fisher and were added at the following final concentrations: for *E. coli*, 30 μg/mL Tmp, 150 μg/mL streptomycin (Sm), 15 μg/mL gentamicin (Gnt), and 100 μg/mL Amp; and for *B. thailandensis*, 100 μg/mL Tmp, 50 μg/mL tetracycline (Tet), and 500 μg/mL kanamycin (Kan). *SI Appendix*, Table S1 lists all bacterial strains, gene deletion mutants, insertional mutants, and reporter strains constructed and/or used in this study.

HiTES. To commence the screen, the *B. thailandensis* reporter strain from an LB agar plate was used to inoculate 5 mL LB-MOPS medium in a sterile 14-mL bacterial culture tube. The culture was grown overnight at 30 °C/250 rpm. After 12 to 16 h, its optical density at 600 nm (OD_{600}) was determined on a Cary 60 UV-visible spectrophotometer (Agilent). The culture was diluted into 200 mL LB-MOPS to give a final OD_{600} of 0.05. Subsequently, a volume of 50 μL was dispensed into each of six sterile, 384-well plates (Corning) using a MultiFlo Microplate Dispenser (Biotek). Candidate elicitors were added to the plates using a CyBi-Well automated liquid transfer robot (CyBio). Each well was supplemented with 0.2 μL compound from the FDA-approved drug library (Enzo Scientific), which comprises 770 molecules. The compounds were dispensed into columns 3 through 22 on each plate. Columns 2 and 23 contained the negative control (the reporter strain being tested in the absence of any compounds), and columns 1 and 24 contained the positive control (strain *btaK-lacZ*, which is expressed at high cell densities). Each assay was carried out in duplicate. After addition of bacteria and candidate elicitors, each plate was covered with a Breathe-Easy sealing membrane (Sigma-Aldrich) and cultured at 30 °C/250 rpm in a Multitron Shaker (Infors) equipped with green sealing trays. To maintain constant humidity, several 1-L Erlenmeyer flasks containing 200 mL sterile water were also placed inside the shaker. After 12 h, the plates were removed from the shaker. The β-Glo reagent (Promega) was used to monitor LacZ activity. The reagent was diluted 2:1 with water. Then each well was supplemented with 15 μL diluted β-Glo reagent using the MultiFlo automated dispenser, manually shaken to mix, and incubated in the dark at room temperature for 45 min. Total end-point luminescence was then determined on a Synergy H1MF plate reader (Biotek).

The same screen was also carried out in an identical fashion in clear-bottom 384-well plates. After 12 h incubation, OD_{600} (rather than luminescence) was determined. Note that the luminescence output was not normalized for OD_{600} in Fig. 1*B*.

Dose–Response Analysis. Hit validation by LacZ assays and dose–response analysis focused on pip, cephalosporins, ciprofloxacin, econazole, sertraline, cinacalcet, and thioridazine. A *malA-lacZ* translational reporter from an LB agar plate was used to inoculate 5 mL LB-MOPS in a sterile 14-mL bacterial culture tube. After 12 h, OD_{600} was determined and the culture diluted to an initial OD_{600} of 0.05 in a 50-mL Erlenmeyer flask containing 10 mL LB-MOPS. The compound of interest was added from a stock generated in dimethyl sulfoxide (DMSO). A control containing only DMSO was also included. Assays were typically carried out in three biological replicates. A positive control culture, *btaK-lacZ* in the absence of any compounds, was grown in parallel as well. The cultures were grown at 30 °C/200 rpm. After 12 h, 65 μL was removed from each flask, dispensed into a sterile, white 96-well plate (Corning), and supplemented with 35 μL 2:1 diluted β-Glo reagent. The plate was incubated in the dark at room temperature for 45 min. End-point luminescence was measured on a H1MF plate reader.

For growth-inhibition assays, the same cultures were grown at 30 °C/200 rpm for 24 h. OD_{600} was determined in clear-bottom 96-well plates.

To obtain EC_{50} and IC_{50} values, the averaged luminescence output (used to determine LacZ activity) or OD_{600} was plotted against the concentration of the inhibitor. The data were fit to a dose–response curve using GraphPad Prism software.

Creation of Site-Specific Deletion Mutants. All deletion mutants were constructed by natural competence transformation with linear DNA fragments (78), which were created by joining three fragments corresponding to upstream and downstream 1-kb regions flanking the gene to be deleted and the Kan or Tet resistance markers (*kan*, *tet*). Competent *B. thailandensis* cells were generated by growing the bacteria overnight in 5-mL low-salt LB medium at 37 °C/200 rpm. The overnight culture was used to inoculate 3 mL M63 medium in a 14-mL sterile culture tube grown at 37 °C/200 rpm. After ~10 h, the cells were pelleted by centrifugation at 12,000 × *g* for 2 min, and the supernatant was discarded. The cells were resuspended in 100 μL M63 medium, and a 50 μL suspension was transferred into a sterile 1.5-mL Eppendorf tube. A total of ~500 ng linear DNA fragment was mixed with the cells by gently tapping the tube, and the resulting mixture was incubated at room temperature for 30 min. The mixture was then transferred into 2 to 3 mL of M63 medium in a 14-mL culture tube and grown at 37 °C/200 rpm overnight. The overnight culture was pelleted by centrifugation,

and the cells were resuspended in ~80 μL M63 medium and plated on low-salt LB agar supplemented with the appropriate antibiotic(s). The plate was then incubated at 37 °C for 24 h or until colonies developed. The mutant colonies were verified by PCR and sequencing. The primers used to generate deletion mutants are listed in *SI Appendix*, Table S2.

Fluorescent Dye–Based ROS Detection. Chloromethal-H_2DCFDA (Invitrogen) was used to detect ROS. Flask cultures of *B. thailandensis* were prepared as described above (see *Dose–Response Analysis* section). The cultures were grown at 30 °C/200 rpm for ~10 h with DMSO or 10 μM pip to an OD_{600} ~1. Dye was added to the culture to a final concentration of 10 μM. Cultures were then grown at 30 °C/200 rpm in the dark in a humidity-controlled Multitron Shaker for 2 h. Then, 100 to 200 μL of each culture was spun down and resuspended in 100 μL 1× phosphate-buffered saline (PBS) solution. Fluorescence emission was measured using a Biotek H1F microplate reader with excitation wavelength (λ_{ex}) set to 495 nm and emission wavelength (λ_{em}) set to 525 nm. The fluorescence intensities measured were normalized for OD_{600}.

PFGE. PFGE was carried out as reported with minor modifications (79). Flask cultures of *B. thailandensis* were prepared as described above. The cultures were then grown at 30 °C/200 rpm for 12 h with DMSO (control) or 10 μM pip. OD_{600} for each culture was determined, and cells corresponding to 1 mL of OD_{600} ~3 were collected. Cell pellets were washed twice in 1 mL ice-cold TEN buffer (50 mM Tris·HCl, pH 8.0, 50 mM EDTA, 100 mM NaCl) and resuspended in 500 μL TEN buffer. The resuspension was mixed with 500 μL 2% low-melting-point agarose and then added to sealed PFGE plug molds. Plugs were first lysed at 37 °C for 2 to 3 h in TEN buffer then supplemented with 250 μg/mL lysozyme. They were then mixed with 1 unit/mL proteinase K in NDS buffer (0.5 M EDTA, 10 mM Tris, 0.6 mM NaOH, 34 mM *N*-lauryl sarcosine, pH 8.0) and lysed at 55 °C overnight. The plugs were rinsed several times with TE buffer (20 mM Tris pH 8.0, 50 mM EDTA) and stored at 4 °C in TE buffer. PFGE was performed using the CHEF-III DR system (Bio-Rad) in a 0.5% agarose gel for 72 h at 3 V, with an initial switch time of 60 s and a final switch time of 120 s and with the running buffer temperature set to 10 to 16 °C. PFGE gels were stained with ethidium bromide for 20 to 30 min with shaking at room temperature and digitally photographed.

TUNEL Assay. Labeling of DNA fragments was performed with the Apo-Direct Kit (BD Bioscience), which employs fluorescein isothiocyanate (FITC)-conjugated deoxyuridine triphosphate (FITC-dUTP) for staining. Flask cultures of *B. thailandensis* were prepared as described above (see *Dose–Response Analysis* section). The cultures were then grown at 30 °C/200 rpm for 12 h with DMSO (control) or 10 μM pip. OD_{600} was determined, and ~10^6 cells were collected for each sample, washed once, and resuspended in 500 μL cold, filtered 1× PBS, pH 7.2 (Fisher). One mL 4% (wt/vol) paraformaldehyde in 1× PBS buffer (Fisher) was added to each sample, which was then incubated on ice for 30 min. Cells were spun down, washed, and resuspended in 250 μL cold 1× PBS. One mL ice-cold 70% ethanol was then added to each sample, and the samples were stored at −20 °C overnight.

For staining, samples were spun down, and ethanol was removed by decanting. They were washed twice in 1 mL wash buffer (kit component). The buffer was removed by aspiration after the second wash and the samples resuspended in 50 μL staining solution (kit component, includes reaction buffer, FITC-dUTP, and deoxynucleotidyl transferase) then incubated for 60 min at 37 °C with shaking. To stop the staining reaction, 1 mL rinse buffer (kit component) was added to each sample. Cells were spun down, rinsed again, resuspended in 1 mL 1× PBS buffer, and analyzed using the BD LSRII flow cytometer (BD Biosciences). A 488-nm argon laser was used for excitation, and a 525- to 550-nm band pass filter was used for FITC fluorescence detection. At least 50,000 cells were collected for each sample. Percent positive cells were determined and reflect the number of TUNEL-positive cells exceeding the fluorescence of 99% of untreated cells.

RT-qPCR. Flask cultures of *B. thailandensis* were prepared as described above (see *Dose–Response Analysis* section). They were then grown at 30 °C/200 rpm for 12 h with DMSO (control) or 10 μM pip. The OD_{600} for each culture was determined, and 50 to 100 μL of each culture, which corresponded to 5 × 10^8 cells, was dispensed into a 1.5-mL RNase-free Eppendorf tube, and the cells were pelleted by centrifugation at 12,000 × *g* for 3 min. The supernatant was discarded, the cells were immediately frozen in liquid N_2 for 5 min, and the samples were then stored at −80 °C. RNA isolation was carried out using the RNeasy kit (Qiagen). Any contaminating DNA was removed from the samples using the DNA-free kit (Ambion). RNA integrity was confirmed by gel electrophoresis. Finally, the RNA was converted into cDNA using the iScript kit (Life Technologies) with random hexamers as primers and 100 to 200 ng of each RNA sample as the template.

RT-qPCR primers (*SI Appendix*, Table S2) were designed using the Primer3-Plus online tool (https://www.bioinformatics.nl/cgi-bin/primer3plus/primer3plus.cgi) to give an amplicon length of 120 to 150 bp and a melting temperature of 60 °C. The genomic DNA of *B. thailandensis* was isolated using the Wizard genomic DNA purification kit (Promega) and used as the template to obtain each amplicon, which was then purified and quantified. A series of standards were generated for each amplicon ranging from ~2 pg/μL down to ~200 attograms (ag)/μL in four successive 10-fold dilution steps and used in quantification. qPCR analysis was performed on a CFX96 real-time PCR detection system (Bio-Rad). The reaction was carried out in hard-shell, clear 96-well qPCR plates and utilized the iTaq Universal SYBR green Supermix (Bio-Rad). Each well contained 8 μL iTaq Supermix, 1 μL standard DNA or cDNA, 1 μL of each primer, and 5 μL nuclease-free water. The PCR cycle consisted of a 1-min incubation (95 °C) followed by 42 cycles of a two-step amplification protocol (5 s at 95 °C, then 30 s at annealing/extension temperature). A single species was observed for all experiments reported.

To determine the levels of each transcript, the quantification cycle (C_q) was determined from triplicate experiments and then converted to amplicon concentration using the standard curve. The resulting value was normalized for total cell number determined in the RNA isolation step and further normalized to the DMSO control sample to give the fold change for that amplicon as a function of pip.

Detection of Malleicyprol by HPLC–MS. Flask cultures were prepared in an identical fashion as described for luminescence assays above (see *Dose–Response Analysis* section). For detection of malleilactone, to which malleicyprol spontaneously converts, the cultures were grown for 24 h at 30 °C/200 rpm. Each culture was then extracted with 20 mL ethyl acetate. The organic layer was dried in vacuo, dissolved in 400 to 1,000 μL MeOH, filtered, and then analyzed by low-resolution HPLC–MS, which was performed on a 1260 Infinity series HPLC system (Agilent) equipped with an automated liquid sampler, a diode array detector, and a 6120 series electrospray ionization mass spectrometer using an analytical Luna C18 column (5 μm, 4.6 × 100 mm; Phenomenex) operating at 0.5 mL/min. Compounds were resolved with an isocratic step with 25% acetonitrile (MeCN) in H_2O over 5 min followed by a gradient of 25 to 100% MeCN over 27 min. Both MeCN and H_2O contained 0.1% (vol/vol) formic acid. Malleilactone production was monitored at 380 nm. The data were routinely normalized for OD_{600}. Note that malleicyprol is secreted; it can therefore be extracted from filtered culture supernatant or by directly subjecting cultures to ethyl acetate extraction.

Complementation Experiments. Expression vector pSCrhaB2 was kindly provided by Josephine R. Chandler (Department of Molecular Biosciences, University of Kansas, Lawrence, KS) (80, 81). Genes coding for *oxyR* and *soxR* were PCR-amplified with primers listed in *SI Appendix*, Table S2. The fragments were digested with NheI/HindIII or KpnI/SalI and introduced into pSCrhaB2, which had been digested with the same enzymes, using the HiFi DNA Assembly Master Mix (New England Biolabs [NEB]) to give pSC-oxyR and pSC-soxR. The plasmid was then introduced into the *ΔoxyR* or *ΔsoxR* mutants by conjugation, and transformants were selected on LB-Tmp-Sm plates. Overnight cultures were diluted to an initial OD_{600} of 0.05 and grown to exponential phase (OD_{600} ~0.5), at which point 0.2% rhamnose was added. The induced cultures were grown at 37 °C/200 rpm for 24 h and subsequently extracted with 20 mL ethyl acetate. The organic layer was isolated, dried completely, and the residue was dissolved in MeOH and subsequently analyzed by HPLC–MS as described in the preceding paragraph.

Transcription Reporter Assay. pJN105 and pQF50 vectors were kindly provided by Josephine R. Chandler (Department of Molecular Biosciences, University of Kansas, Lawrence, KS), and the transcription reporter assay was carried out as previously reported, with modifications (59). To generate pJN105-oxyR for recombinant *oxyR* expression in *E. coli*, *oxyR* was PCR-amplified using primers listed in *SI Appendix*, Table S2. It was then digested with NheI/SpeI (NEB) and ligated into NheI/SpeI-treated pJN105 using the HiFi DNA Assembly Master Mix to give pJN105-oxyR. To generate the *E. coli* P_{malR}-*lacZ* expression vector pQF50-P_{malR}, the region upstream of *malR* extending from positions −1 to −670 with respect to the translational start site was PCR-amplified (*SI Appendix*, Table S2) and treated with NcoI/HindIII (NEB). The fragment was introduced into NcoI-HindIII–digested pQF50 using HiFi DNA Assembly Master Mix to give pQF50-P_{malR}. pQF50-P_{ahpC} was constructed in an analogous manner.

To assess *oxyR*-mediated *malR* expression in recombinant *E. coli*, we used *E. coli* MG4 strain with arabinose-inducible *oxyR* (pJN105-oxyR) and pQF50-PmalR.

Overnight cultures were used as starters by diluting them to an OD_{600} of 0.05. L-Arabinose was added to final concentrations indicated to induce expression, when OD_{600} reached 0.5. After 2 h at 37 °C with shaking, LacZ assays were carried out with the β-Glo reagent as described above (see *Dose–Response Analysis* section).

Cloning, Expression, and Purification of OxyR. To prepare *B. thailandensis* OxyR for the electrophoretic mobility shift assay (EMSA), *oxyR* was PCR-amplified (*SI Appendix*, Table S2), digested with BamHI/SalI, and the fragment was introduced into BamHI/SalI-treated pET-28b(+) using the HiFi DNA Assembly Master Mix to give pET-28b(+)-oxyR. The sequence-validated plasmid was used to transform *E. coli* BL21(DE3) cells for expression.

A 14-mL sterile culture tube containing 5 mL LB broth supplemented with Kan was inoculated with a single colony of *E. coli* BL21(DE3) cells carrying pET-28b(+)-oxyR. The 50mL culture was grown at 37 °C/200 rpm for 12 h, at which point 500 μL (1% vol/vol) were used to inoculate 50 mL LB-Kan in a 250-mL Erlenmeyer flask. These intermediate cultures were grown overnight at 37 °C/200 rpm and subsequently used to inoculate 1.6 L LB-Kan in 4-L Erlenmeyer flasks with 1% (vol/vol) of the intermediate culture. The large culture was grown at 37 °C/200 rpm to an OD_{600} ~0.6, cooled in an ice bath for 5 to 10 min, and then supplemented with a final concentration of 0.5 mM IPTG. After shaking at 18 °C/180 rpm for 20 h, the cells were harvested by centrifugation (8,000 × *g*, 15 min, 4 °C), frozen, and stored at −80 °C. Typically, a yield of 5.8 g of cells per liter culture was obtained.

Purification of OxyR was carried out at 4 °C. The lysis buffer consisted of 50 mM Tris, 50 mM NaCl, 5 mM imidazole, 5% glycerol, pH 7.8, and 1 mM β-mercaptoethanol. The cell pellet was resuspended in lysis buffer (5 mL/g) in a 250-mL beaker. The suspension was supplemented with protease inhibitor mixture (0.1% vol/vol), phenylmethylsulfonyl fluoride (PMSF, 0.25 mM), lysozyme (1 mg/mL), and DNase I (10 U/mL). Subsequently, the suspension was stirred for 30 min and sonicated on ice for 2 min in 15 s on/15 s off cycles at 30% power. The sonication cycle was repeated after the suspension rested on ice for 5 min, and then cell debris was pelleted via centrifugation (32,000 × *g*, 1 h, 4 °C). PMSF (0.25 mM final concentration) was added to the crude extract, which was then loaded onto a nickel metal affinity column (15 mL) that had been equilibrated with lysis buffer. The column was washed with 10 CV lysis buffer and 4 CV wash buffer (50 mM Tris, 50 mM NaCl, 30 mM imidazole, 5% glycerol, pH 7.8, 1 mM β-mercaptoethanol, and 0.25 mM PMSF). Finally, the protein was eluted with 4 CV elution buffer (50 mM Tris, 50 mM NaCl, 300 mM imidazole, 5% glycerol, pH 7.8, 1 mM β-mercaptoethanol, and 0.25 mM PMSF). His_6-OxyR was buffer-exchanged on a Sephadex G-25 column (~20 mL, d = 1.25 cm, l = 25 cm) that had been equilibrated with G25 buffer (50 mM Tris, 100 mM KCl, 5% glycerol, pH 7.8). The desired protein fractions were pooled, analyzed by SDS-PAGE and UV-vis spectroscopy, flash frozen in liquid N_2, and stored at −80 °C. A typical yield was 10 mg protein per liter of culture.

EMSA. The promoter fragment of *malR* and *ahpC* were PCR-amplified from *B. thailandensis* genomic DNA (*SI Appendix*, Table S2). All PCR fragments were purified with QIAquick Gel Extraction Kit (Qiagen). The mutated promoter fragment was synthesized by Genewiz. A total of 15 μL EMSA reaction solutions were prepared by mixing 300 ng DNA fragment (P_{malR}, $P_{malR\text{-}mut}$, P_{ahpC}, or random fragment), various amounts of the proteins (His_6-OxyR or bovine serum albumin [BSA]), and G25 buffer. Reaction solutions were incubated for 30 min at room temperature. The protein–DNA mixtures were resolved on a 1.5% agarose gel, which was then stained with 0.5 μg/mL ethidium bromide for 20 min and visualized with a Gel Doc EZ System (Bio-Rad).

Data Availability. All study data are included in the article and/or *SI Appendix*.

ACKNOWLEDGMENTS. We thank Professor Virginia A. Zakian for use of her PFGE setup as well as the NIH for Grant DP2-AI-124786 (awarded to M.R.S.) and a graduate fellowship from the the China Scholarship Council (to A.L.) for financial support.

1. D. J. Newman, G. M. Cragg, Natural products as sources of new drugs over the nearly four decades from 01/1981 to 09/2019. *J. Nat. Prod.* **83**, 770–803 (2020).
2. J. Clardy, M. A. Fischbach, C. R. Currie, The natural history of antibiotics. *Curr. Biol.* **19**, R437–R441 (2009).
3. M. Nett, H. Ikeda, B. S. Moore, Genomic basis for natural product biosynthetic diversity in the actinomycetes. *Nat. Prod. Rep.* **26**, 1362–1384 (2009).
4. S. D. Bentley *et al.*, Complete genome sequence of the model actinomycete Streptomyces coelicolor A3(2). *Nature* **417**, 141–147 (2002).
5. H. Ikeda *et al.*, Complete genome sequence and comparative analysis of the industrial microorganism *Streptomyces avermitilis*. *Nat. Biotechnol.* **21**, 526–531 (2003).
6. M. Oliynyk *et al.*, Complete genome sequence of the erythromycin-producing bacterium *Saccharopolyspora erythraea* NRRL23338. *Nat. Biotechnol.* **25**, 447–453 (2007).
7. G. C. A. Amos *et al.*, Comparative transcriptomics as a guide to natural product discovery and biosynthetic gene cluster functionality. *Proc. Natl. Acad. Sci. U.S.A.* **114**, E11121–E11130 (2017).
8. K. Ochi, T. Hosaka, New strategies for drug discovery: Activation of silent or weakly expressed microbial gene clusters. *Appl. Microbiol. Biotechnol.* **97**, 87–98 (2013).
9. P. J. Rutledge, G. L. Challis, Discovery of microbial natural products by activation of silent biosynthetic gene clusters. *Nat. Rev. Microbiol.* **13**, 509–523 (2015).
10. V. Yoon, J. R. Nodwell, Activating secondary metabolism with stress and chemicals. *J. Ind. Microbiol. Biotechnol.* **41**, 415–424 (2014).
11. D. Mao, B. K. Okada, Y. Wu, F. Xu, M. R. Seyedsayamdost, Recent advances in activating silent biosynthetic gene clusters in bacteria. *Curr. Opin. Microbiol.* **45**, 156–163 (2018).
12. S. Rigali, S. Anderssen, A. Naômé, G. P. van Wezel, Cracking the regulatory code of biosynthetic gene clusters as a strategy for natural product discovery. *Biochem. Pharmacol.* **153**, 24–34 (2018).
13. H. Ren, B. Wang, H. Zhao, Breaking the silence: New strategies for discovering novel natural products. *Curr. Opin. Biotechnol.* **48**, 21–27 (2017).
14. M. R. Seyedsayamdost, High-throughput platform for the discovery of elicitors of silent bacterial gene clusters. *Proc. Natl. Acad. Sci. U.S.A.* **111**, 7266–7271 (2014).
15. F. Xu *et al.*, A genetics-free method for high-throughput discovery of cryptic microbial metabolites. *Nat. Chem. Biol.* **15**, 161–168 (2019).
16. M. R. Seyedsayamdost, Towards a global picture of bacterial secondary metabolism. *J. Ind. Microbiol. Biotechnol.* **46**, 301–311 (2019).
17. A. Craney, C. Ozimok, S. M. Pimentel-Elardo, A. Capretta, J. R. Nodwell, Chemical perturbation of secondary metabolism demonstrates important links to primary metabolism. *Chem. Biol.* **19**, 1020–1027 (2012).
18. Y. Imai, S. Sato, Y. Tanaka, K. Ochi, T. Hosaka, Lincomycin at subinhibitory concentrations potentiates secondary metabolite production by *Streptomyces* spp. *Appl. Environ. Microbiol.* **81**, 3869–3879 (2015).
19. A. Li *et al.*, Multi-omic analyses provide links between low-dose antibiotic treatment and induction of secondary metabolism in *Burkholderia thailandensis*. *mBio* **11**, e03210-19 (2020).
20. E.-B. Goh *et al.*, Transcriptional modulation of bacterial gene expression by subinhibitory concentrations of antibiotics. *Proc. Natl. Acad. Sci. U.S.A.* **99**, 17025–17030 (2002).
21. J. Davies, G. B. Spiegelman, G. Yim, The world of subinhibitory antibiotic concentrations. *Curr. Opin. Microbiol.* **9**, 445–453 (2006).
22. A. Fajardo, J. L. Martínez, Antibiotics as signals that trigger specific bacterial responses. *Curr. Opin. Microbiol.* **11**, 161–167 (2008).
23. D. I. Andersson, D. Hughes, Microbiological effects of sublethal levels of antibiotics. *Nat. Rev. Microbiol.* **12**, 465–478 (2014).
24. B. K. Okada, M. R. Seyedsayamdost, Antibiotic dialogues: Induction of silent biosynthetic gene clusters by exogenous small molecules. *FEMS Microbiol. Rev.* **41**, 19–33 (2017).
25. M. A. Kohanski, D. J. Dwyer, J. J. Collins, How antibiotics kill bacteria: From targets to networks. *Nat. Rev. Microbiol.* **8**, 423–435 (2010).
26. P. J. Brett, D. DeShazer, D. E. Woods, Note: *Burkholderia thailandensis* sp. nov., a *Burkholderia pseudomallei*-like species. *Int. J. Syst. Evol. Microbiol.* **48**, 317–320 (1998).
27. X. Liu, Y.-Q. Cheng, Genome-guided discovery of diverse natural products from Burkholderia sp. *J. Ind. Microbiol. Biotechnol.* **41**, 275–284 (2014).
28. T. Nguyen *et al.*, Exploiting the mosaic structure of trans-acyltransferase polyketide synthases for natural product discovery and pathway dissection. *Nat. Biotechnol.* **26**, 225–233 (2008).
29. L. Vial *et al.*, *Burkholderia pseudomallei, B. thailandensis*, and *B. ambifaria* produce 4-hydroxy-2-alkylquinoline analogues with a methyl group at the 3 Position that is required for quorum-sensing regulation. *J. Bacteriol.* **190**, 5339–5352 (2008).
30. M. R. Seyedsayamdost *et al.*, Quorum-sensing-regulated bactobolin production by *Burkholderia thailandensis* E264. *Org. Lett.* **12**, 716–719 (2010).
31. G. Carr, M. R. Seyedsayamdost, J. R. Chandler, E. P. Greenberg, J. Clardy, Sources of diversity in bactobolin biosynthesis by *Burkholderia thailandensis* E264. *Org. Lett.* **13**, 3048–3051 (2011).
32. B. K. Okada, Y. Wu, D. Mao, L. B. Bushin, M. R. Seyedsayamdost, Mapping the trimethoprim-induced secondary metabolome of *B. thailandensis*. *ACS Chem. Biol.* **11**, 2124–2130 (2016).
33. J. B. Biggins, M. A. Ternei, S. F. Brady, Malleilactone, a polyketide synthase-derived virulence factor encoded by the cryptic secondary metabolome of *Burkholderia pseudomallei* group pathogens. *J. Am. Chem. Soc.* **134**, 13192–13195 (2012).
34. J. Franke, K. Ishida, C. Hertweck, Genomics-driven discovery of burkholderic acid, a noncanonical, cryptic polyketide from human pathogenic *Burkholderia* species. *Angew. Chem. Int. Ed. Engl.* **51**, 11611–11615 (2012).
35. F. Trottmann *et al.*, A cyclopropanol warhead in malleicyprol confers virulence of human- and animal-pathogenic *Burkholderia* species. *Angew. Chem. Int. Ed. Engl.* **58**, 14129–14133 (2019).
36. J.-D. Park *et al.*, Thailandenes, cryptic polyene natural products isolated from *Burkholderia thailandensis* using phenotype-guided transposon mutagenesis. *ACS Chem. Biol.* **15**, 1195–1203 (2020).

37. J. Franke, K. Ishida, M. Ishida-Ito, C. Hertweck, Nitro versus hydroxamate in siderophores of pathogenic bacteria: Effect of missing hydroxylamine protection in malleobactin biosynthesis. *Angew. Chem. Int. Ed. Engl.* **52**, 8271–8275 (2013).
38. D. Mao, A. Yoshimura, R. Wang, M. R. Seyedsayamdost, Reporter-Guided transposon mutant selection for activation of silent gene clusters in *Burkholderia thailandensis*. *ChemBioChem* **21**, 1826–1831 (2020).
39. K. Blin *et al*., antiSMASH 5.0: updates to the secondary metabolite genome mining pipeline. *Nucleic Acids Res.* **47**, W81–W87 (2019).
40. L. A. Gallagher *et al*., Sequence-defined transposon mutant library of *Burkholderia thailandensis*. *mBio* **4**, e00604–e00613 (2013).
41. E. T. Zeiser *et al*., "Switching partners": Piperacillin-avibactam is a highly potent combination against multidrug-resistant *Burkholderia cepacia* complex and *Burkholderia gladioli* cystic fibrosis isolates. *J. Clin. Microbiol.* **57**, e00181–e19 (2019).
42. N. J. White *et al*., Halving of mortality of severe melioidosis by ceftazidime. *Lancet* **334**, 697–701 (1989).
43. C. Miller *et al*., SOS response induction by β-lactams and bacterial defense against antibiotic lethality. *Science* **305**, 1629–1631 (2004).
44. M. A. Kohanski, D. J. Dwyer, B. Hayete, C. A. Lawrence, J. J. Collins, A common mechanism of cellular death induced by bactericidal antibiotics. *Cell* **130**, 797–810 (2007).
45. D. J. Dwyer *et al*., Antibiotics induce redox-related physiological alterations as part of their lethality. *Proc. Natl. Acad. Sci. U.S.A.* **111**, E2100–E2109 (2014).
46. P. Belenky *et al*., Bactericidal antibiotics induce toxic metabolic perturbations that lead to cellular damage. *Cell Rep.* **13**, 968–980 (2015).
47. J. A. Imlay, Pathways of oxidative damage. *Annu. Rev. Microbiol.* **57**, 395–418 (2003).
48. J. A. Imlay, The molecular mechanisms and molecular consequences of oxidative stress: Lessons from a model bacterium. *Nat. Rev. Microbiol.* **11**, 433–454 (2013).
49. M. Gu, J. A. Imlay, The SoxRS response of *Escherichia coli* is directly activated by redox-cycling drugs rather than by superoxide. *Mol. Microbiol.* **79**, 1136–1150 (2011).
50. R. Sheplock, D. A. Recinos, N. Mackow, L. E. P. Dietrich, M. Chander, Species-specific residues calibrate SoxR sensitivity to redox-active molecules. *Mol. Microbiol.* **87**, 368–381 (2013).
51. D. R. Peralta *et al*., Enterobactin as part of the oxidative stress response repertoire. *PLoS One* **11**, e0157799 (2016).
52. D. J. Dwyer, D. M. Camacho, M. A. Kohanski, J. M. Callura, J. J. Collins, Antibiotic-induced bacterial cell death exhibits physiological and biochemical hallmarks of apoptosis. *Mol. Cell* **46**, 561–572 (2012).
53. Y. Gavrieli, Y. Sherman, S. A. Ben-Sasson, Identification of programmed cell death in situ via specific labeling of nuclear DNA fragmentation. *J. Cell Biol.* **119**, 493–501 (1992).
54. N. Joshi, S. G. Grant, "DNA double-strand break damage and repair assessed by pulsed-field gel electrophoresis" in *Molecular Toxicology Protocols*, P. Keohavong, S. G. Grant, Eds. (Methods in Molecular Biology, Humana Press, 2005), pp. 121–129.
55. K. Schlacher, M. F. Goodman, Lessons from 50 years of SOS DNA-damage-induced mutagenesis. *Nat. Rev. Mol. Cell Biol.* **8**, 587–594 (2007).
56. J. A. Imlay, Transcription factors that defend bacteria against reactive oxygen species. *Annu. Rev. Microbiol.* **69**, 93–108 (2015).
57. H. M. Hassan, I. Fridovich, Intracellular production of superoxide radical and of hydrogen peroxide by redox active compounds. *Arch. Biochem. Biophys.* **196**, 385–395 (1979).
58. H. M. Hassan, I. Fridovich, Superoxide radical and the oxygen enhancement of the toxicity of paraquat in *Escherichia coli*. *J. Biol. Chem.* **253**, 8143–8148 (1978).
59. T. T. Truong, M. Seyedsayamdost, E. P. Greenberg, J. R. Chandler, A *Burkholderia thailandensis* acyl-homoserine lactone-independent orphan LuxR homolog that activates production of the cytotoxin malleilactone. *J. Bacteriol.* **197**, 3456–3462 (2015).
60. R. Münch *et al*., Virtual footprint and PRODORIC: An integrative framework for regulon prediction in prokaryotes. *Bioinformatics* **21**, 4187–4189 (2005).
61. B. Zhang *et al*., Molecular mechanisms of Ahpc in resistance to oxidative stress in *Burkholderia thailandensis*. *Front. Microbiol.* **10**, 1483 (2019).
62. D. Romero, M. F. Traxler, D. López, R. Kolter, Antibiotics as signal molecules. *Chem. Rev.* **111**, 5492–5505 (2011).
63. J. M. Stokes, A. J. Lopatkin, M. A. Lobritz, J. J. Collins, Bacterial metabolism and antibiotic efficacy. *Cell Metab.* **30**, 251–259 (2019).
64. M. A. Lobritz *et al*., Antibiotic efficacy is linked to bacterial cellular respiration. *Proc. Natl. Acad. Sci. U.S.A.* **112**, 8173–8180 (2015).
65. T. Dörr *et al*., A cell wall damage response mediated by a sensor kinase/response regulator pair enables beta-lactam tolerance. *Proc. Natl. Acad. Sci. U.S.A.* **113**, 404–409 (2016).
66. S. Utaida, Genome-wide transcriptional profiling of the response of *Staphylococcus aureus* to cell-wall-active antibiotics reveals a cell-wall-stress stimulon. *Microbiology* **149**, 2719–2732 (2003).
67. C. N. Paiva, M. T. Bozza, Are reactive oxygen species always detrimental to pathogens. *Antioxid. Redox Signal.* **20**, 1000–1037 (2014).
68. J. A. Imlay, Where in the world do bacteria experience oxidative stress. *Environ. Microbiol.* **21**, 521–530 (2019).
69. T. Beites *et al*., Crosstalk between ROS homeostasis and secondary metabolism in *S. natalensis* ATCC 27448: Modulation of pimaricin production by intracellular ROS. *PLoS One* **6**, e27472 (2011).
70. X. Liu *et al*., OxyR is a key regulator in response to oxidative stress in *Streptomyces avermitilis*. *Microbiology* **162**, 707–716 (2016).
71. J. D. Helmann *et al*., The global transcriptional response of B. Subtilis to peroxide stress is coordinated by three transcription factors. *J. Bacteriol.* **185**, 243–253 (2003).
72. J. Mostertz, C. Scharf, M. Hecker, G. Homuth, Transcriptome and proteome analysis of *Bacillus subtilis* gene expression in response to superoxide and peroxide stress. *Microbiology* **150**, 497–512 (2004).
73. M. A. Fischbach, C. T. Walsh, Assembly-line enzymology for polyketide and nonribosomal peptide antibiotics: Logic, machinery, and mechanisms. *Chem. Rev.* **106**, 3468–3496 (2006).
74. S. Kunakom, A. S. Eustáqio, *Burkholderia* as a source of natural products. *J. Nat. Prod.* **82**, 8012–8037 (2019).
75. L. Meier *et al*., Extensive impact of non-antibiotic drugs on human gut bacteria. *Nature* **555**, 523–528 (2018).
76. B. K. Okada, A. Li, M. R. Seyedsayamdost, Identification of the hypertension drug guanfacine as an anti-virulence agent in *Pseudomonas aeruginosa*. *ChemBioChem* **20**, 2005–2011 (2019).
77. J. A. V. Blodgett *et al*., Common biosynthetic origins for polycyclic tetramate macrolactams from phylogenetically diverse bacteria. *Proc. Natl. Acad. Sci. U.S.A.* **107**, 11692–11697 (2010).
78. M. Thongdee *et al*., Targeted mutagenesis of *Burkholderia thailandensis* and *Burkholderia pseudomallei* through natural transformation of PCR fragments. *Appl. Environ. Microbiol.* **74**, 2985–2989 (2008).
79. J. Herschleb, G. Ananiev, D. C. Schwartz, Pulsed-field gel electrophoresis. *Nat. Protoc.* **2**, 677–684 (2007).
80. J. R. Chandler *et al*., Mutational analysis of *Burkholderia thailandensis* quorum sensing and self-aggregation. *J. Bacteriol.* **191**, 5901–5909 (2009).
81. S. T. Cardona, M. A. Valvano, An expression vector containing a rhamnose-inducible promoter provides tightly regulated gene expression in *Burkholderia cenocepacia*. *Plasmid* **54**, 219–228 (2005).